Figure S1

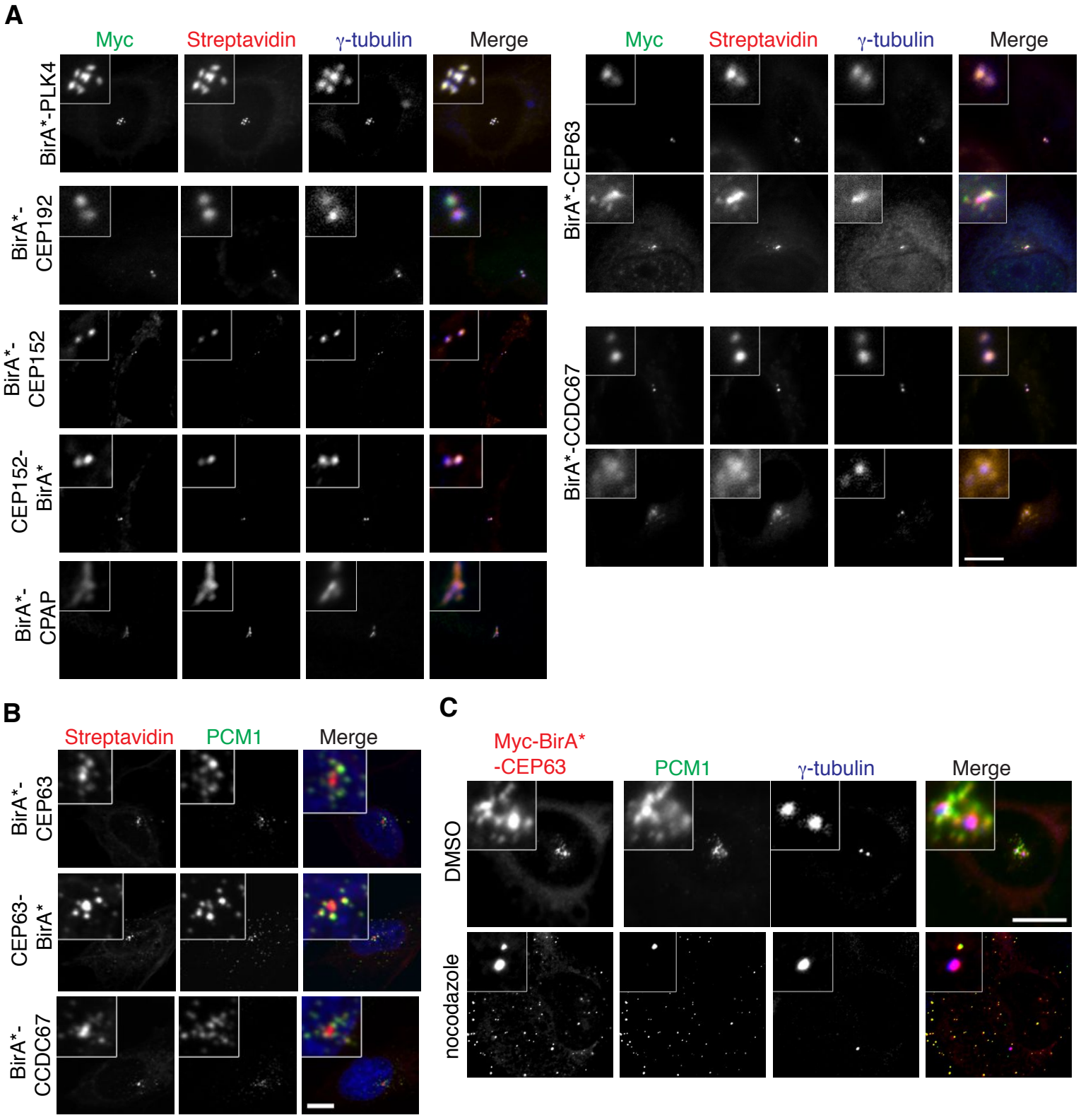
A
Myc
Streptavidin
γ-tubulin
Merge
BirA*-PLK4
BirA*-CEP192
BirA*-CEP152
CEP152-BirA*
BirA*-CPAP
BirA*-CEP63
BirA*-CCDC67
B
Streptavidin
PCM1
Merge
BirA*-CEP63
CEP63-BirA*
BirA*-CCDC67
C
Myc-BirA*-CEP63
PCM1
γ-tubulin
Merge
DMSO
nocodazole

Figure S2

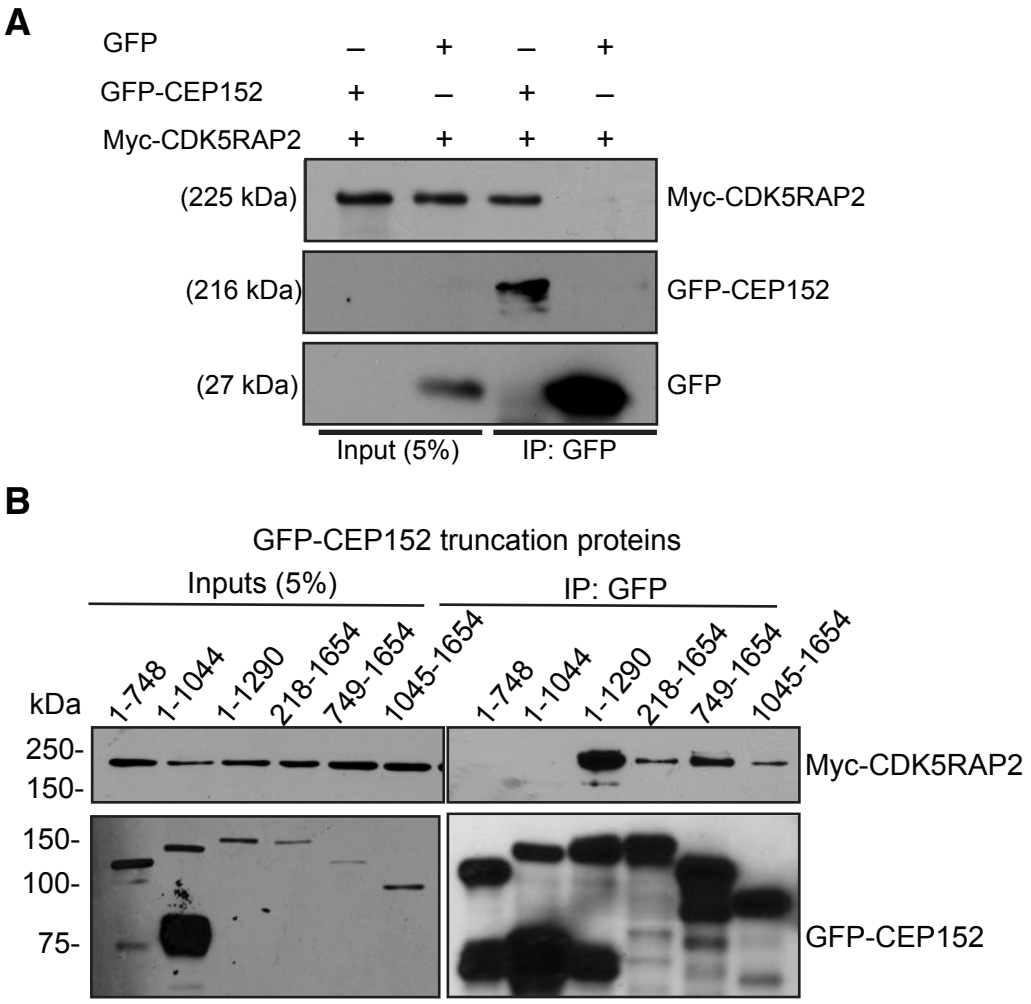
A
GFP
GFP-CEP152
Myc-CDK5RAP2
(225 kDa)
(216 kDa)
(27 kDa)
Myc-CDK5RAP2
GFP-CEP152
GFP
Input (5%)
IP: GFP
B
GFP-CEP152 truncation proteins
Inputs (5%)
IP: GFP
kDa
1-748
1-1044
1-1290
218-1654
749-1654
1045-1654
250-
150-
150-
100-
75-
Myc-CDK5RAP2
GFP-CEP152

Figure S3

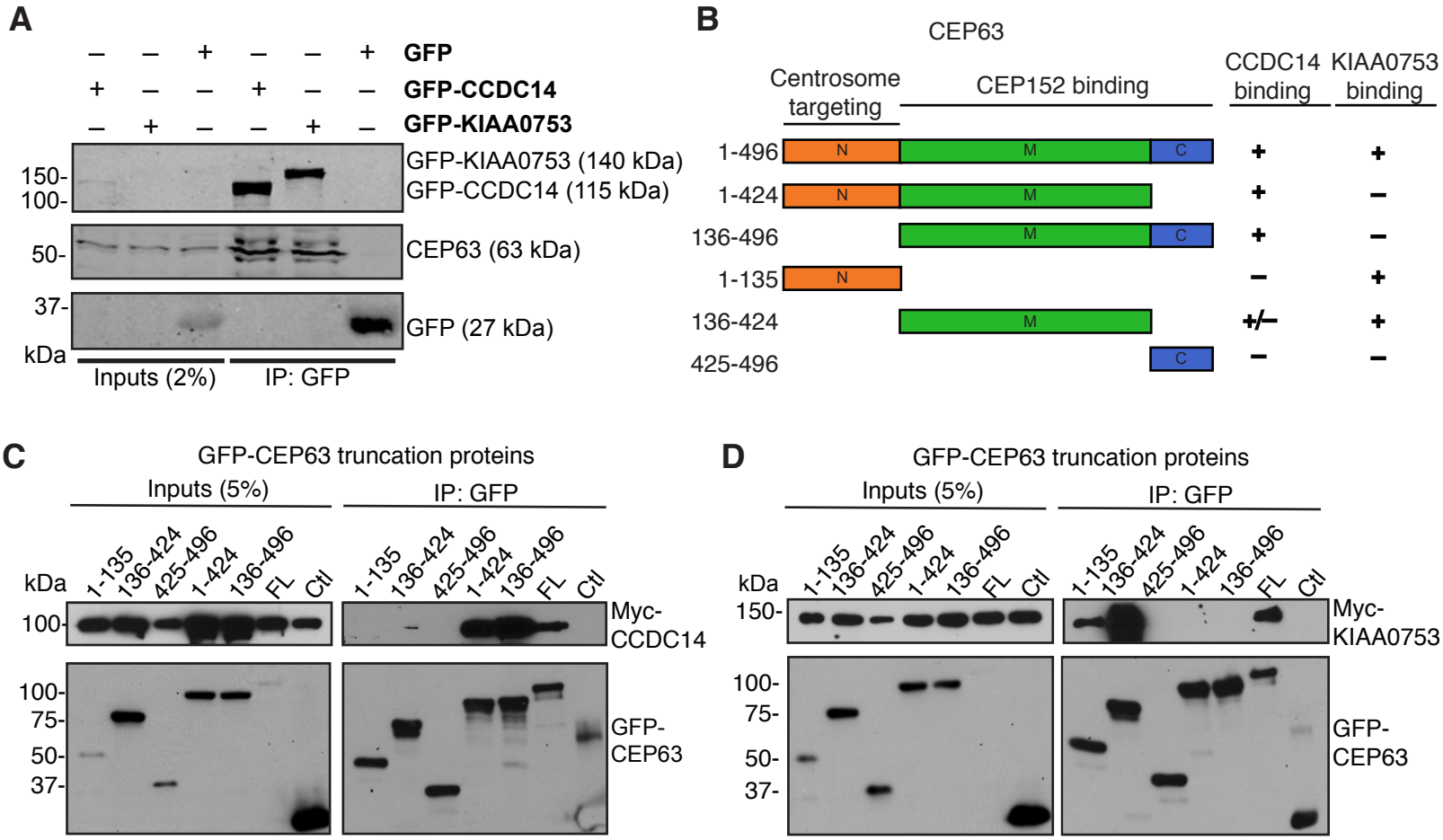
A
– – + – – + GFP
+ – – + – – GFP-CCDC14
– + – – + – GFP-KIAA0753
150-
100-
50-
37-
kDa
GFP-KIAA0753 (140 kDa)
GFP-CCDC14 (115 kDa)
CEP63 (63 kDa)
GFP (27 kDa)
Inputs (2%)
IP: GFP
B
CEP63
Centrosome targeting
CEP152 binding
CCDC14 binding
KIAA0753 binding
1-496
1-424
136-496
1-135
136-424
425-496
N
M
C
+
–
+/–
C
GFP-CEP63 truncation proteins
Inputs (5%)
IP: GFP
kDa
1-135
136-424
425-496
1-424
136-496
FL
Ctl
100-
Myc-CCDC14
100-
75-
50-
37-
GFP-CEP63
150-
Myc-KIAA0753

Figure S4

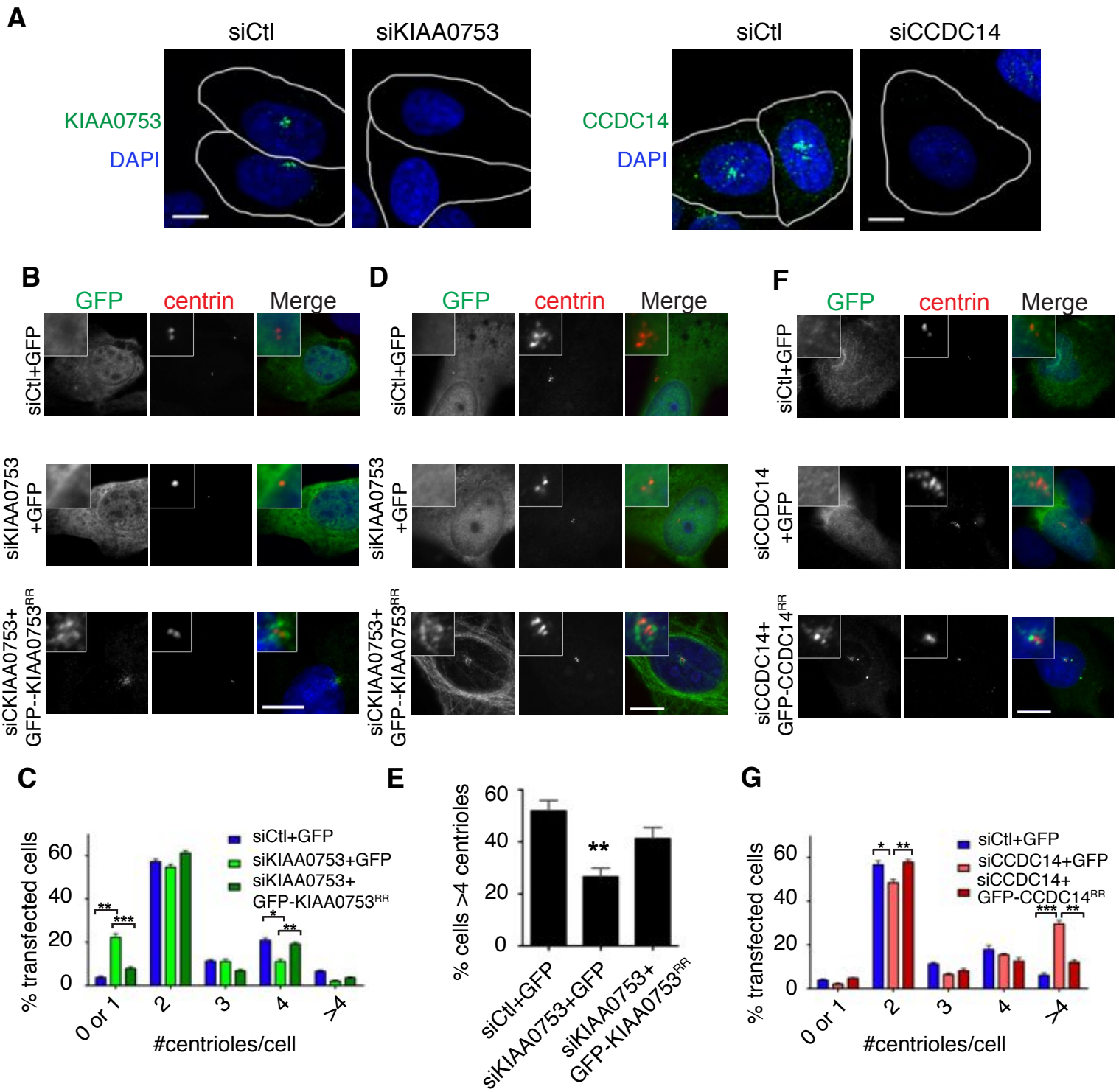
A
siCtl
siKIAA0753
siCtl
siCCDC14
KIAA0753
DAPI
CCDC14
DAPI
B
D
F
GFP
centrin
Merge
siCtl+GFP
siKIAA0753 +GFP
siCCDC14 +GFP
siCKIAA0753+ GFP--KIAA0753RR
siCCDC14+ GFP-CCDC14RR
C
% transfected cells
siCtl+GFP
siKIAA0753+GFP
siKIAA0753+ GFP-KIAA0753RR
0 or 1
2
3
4
>4
#centrioles/cell
E
% cells >4 centrioles
siCtl+GFP
siKIAA0753+GFP
siKIAA0753+ GFP-KIAA0753RR
G
% transfected cells
siCtl+GFP
siCCDC14+GFP
siCCDC14+ GFP-CCDC14RR
#centrioles/cell

Table S1

BirA*-PLK4

Protein	NSAF
PLK4	152
SDCCAG3	1.34
CEP152	1.33
CEP192	1.28
CEP85	1.22
PCNT	1.13
KIAA1671	1.08
NEDD1	1.08
MAGED1	1.03
TTK	0.87
LZTS2	0.79
PLK1	0.78
ALMS1	0.71
USP54	0.77
STIL	0.62
CEP128	0.47
FAM83H	0.46
OFD1	0.43
CSPP1	0.42
DOCK7	0.41
KIF2A	0.35
SPICE1	0.33
PCM1	0.31
CEP350	0.31
ODF2	0.26
MYCBP2	0.22
AZI1	0.21
CEP63	0.21
CDK5RAP2	0.21
FBXW11	0.19
CCDC15	0.18
SASS6	0.18
CEP250	0.18

BirA*-CEP192

Protein	NSAF
CEP192	97
AURKA	3.81
NEDD1	2.71
CACYBP	1.39
CEP85	1.06
PCNT	0.95
ALMS1	0.86
MAGED1	0.82
CYLD	0.69
OFD1	0.60
CEP152	0.56
PCM1	0.51
AZI1	0.50
CEP350	0.37
CEP63	0.37
KIAA1671	0.35
CDK5RAP2	0.31
PLK1S1	0.27
USP42	0.19
TRIM37	0.19
KIAA1731	0.18
SPATA2	0.17
MARK3	0.14

BirA*-CEP63

Protein	NSAF
CEP63	113
PCM1	1.89
AZI1	1.23
CCDC14	1.14
CEP57	0.94
KIAA0753	0.90
OFD1	0.88
PCNT	0.68
CEP152	**0.60**
CEP128	0.56
CSPP1	0.44
KIF7	0.40
CEP350	0.38
ALMS1	0.37
CCDC138	0.37
CEP192	0.26
CEP90	0.26
CEP85	0.24
LZTS2	0.20
UBE20	0.19
APC	0.18
SIPA1L1	0.16
SPICE1	0.16
C2CD3	0.14
NIN	0.13
TNIK	0.11

BirA*-CCDC67

Protein	NSAF
CCDC67	207
IFT20	1.56
PCM1	1.27
CEP85	0.74
CCHCR1	0.59
CCDC57	0.52
CEP152	0.51
SPAG5	0.50
OFD1	0.49
CSPP1	0.47
PRPF4B	0.44
NKTR	0.40
CEP128	0.37
MPHOSPH9	0.26
KIAA1671	0.25
TUBG1	0.23
PCNT	0.22
MAGED1	0.17
AZI1	0.16
CEP63	0.14
CEP192	0.13

BirA*-CPAP

Protein	NSAF
CPAP	91
LRCC40	2.50
CEP55	2.05
AZI1	1.99
NEDD1	1.24
PLK1	1.12
CEP120	1.06
CP110	1.05
CEP85	0.95
CLASP1	0.93
CKAP2	0.84
MIB1	0.69
STIL	0.65
TTK	0.65
LZTS2	0.61
KIAA1671	0.56
CEP97	0.43
IQSEC1	0.30
KIF14	0.29
PCNT	0.26
KIF7	0.25
KIAA0586	0.23
ALMS1	0.22
CEP192	0.21
C2CD3	0.20
ODF2	0.18
CDC7	0.11

CEP152-BirA*

Protein	NSAF
CEP152	22.3
CPAP	2.31
CEP63	1.21
PCNT	0.74
CDK5RAP2	0.59
CEP192	0.51
NEDD1	0.50
GSDMA	0.47
MTHFD1L	0.37
AZI1	0.23
PCM1	0.22
LYAR	0.21
A2ML1	0.20
CEP128	0.11
ALMS1	0.10

BirA*-CEP152

Protein	NSAF
CEP152	60
LYAR	5.78
AZI1	1.73
CEP192	1.08
CEP63	0.93
PCNT	0.54
CEP85	0.25
PCM1	0.23
KIAA0753	0.20
ALMS1	0.12
CEP350	0.11
MYO9A	0.10

Table S2

BirA*-KIAA0753	
Protein	**NSAF**
KIAA0753	280
STIP1	6.63
MAP7D3	2.89
CDK1	1.64
CEP55	1.62
PCM1	1.60
CEP90	1.41
OFD1	1.14
CKAP2	0.98
GTSE1	0.92
STUB1	0.74
PJA2	0.68
ABLIM1	0.65
MPHOSPH9	0.51
CCDC138	0.48
SPAG5	0.41
UBE2O	0.42
PJA1	0.41
MAGED1	0.40
PLK1S1	0.38
MAP7D2	0.35
FGFR1OP	0.33
CEP350	0.32
SQSTM1	0.30
DVL2	0.24
AZI1	0.24
KIAA0586	0.22
CEP72	0.30
CCDC15	0.17
PUM1	0.14
TRIM37	0.13
CP110	0.13
CEP152	0.13
GOPC	0.12
POC5	0.11
ALMS1	0.11
CEP63	0.10
CSPP1	0.10

BirA*-CCDC14	
Protein	**NSAF**
CCDC14	298
STIP1	9.87
CEP55	4.61
CDK1	3.99
ZWINT	2.69
SDCCAG3	2.44
COMMD8	1.91
CEP85	1.87
PCM1	1.62
SKA3	1.45
VCPIP	1.31
THOC7	1.15
OFD1	0.96
FGFR1OP	0.95
HAUS2	0.84
SQTM1	0.79
SPAG5	0.73
HAUS8	0.69
CEP72	0.52
MAGED1	0.43
CNTROB	0.37
CCDC138	0.25
MPHOSPH9	0.25
CCNB2	0.22
TRIM37	0.15
CEP90	0.14
CEP63	0.12

Supplemental Figure and Table Legends

Figure S1, Related to Figure 1. Localization and activity of BirA*-centrosome protein fusions

U2OS cells were transfected with Myc-BirA*-tagged fusions to the following proteins: **(A)** PLK4, CEP192, CEP152, CPAP, CEP63 and CCDC67. After 18 h incubation with biotin, cells were fixed, and stained for Myc-BirA*-fusion proteins with anti-Myc antibody, for biotinylated proteins with fluorescent streptavidin and centrosomes with anti-γ-tubulin antibody. **(B)** U2OS cells were transfected with Myc-BirA*-CEP63, CEP63-Myc-BirA* or Myc-BirA*-CCDC67. After 18 h incubation with biotin, cells were fixed and stained for biotinylated proteins with fluorescent streptavidin and centriolar satellites with anti-PCM1 antibody. **(C)** Microtubule depolymerization results in dispersal of centriolar satellites that are positive for Myc-BirA*-CEP63. U2OS cells were transfected with Myc-BirA*-CEP63. 24 h after transfection, cells treated with DMSO or nocodazole (5 μg/ml) for 3 h, fixed and stained for Myc-BirA*-CEP63 with anti-Myc antibody, centriolar satellites with PCM1 antibody and centrosomes with anti-γ-tubulin antibody. Scale bars = 10 μm, all insets show 4x enlarged centrosomes.

Figure S2, Related to Figure 2. Characterization of CEP152 interaction with CDK5RAP2

(A) Co-immunoprecipitation of Myc-CDK5RAP2 and GFP-CEP152 after co-transfection in HEK293T cells. Complexes were immunoprecipitated with anti-

GFP antibody and co-precipitated proteins were detected with anti-GFP and anti-Myc antibodies. **(B)** GFP-CEP152 truncation constructs were co-transfected with Myc-CDK5RAP2 in HEK293T cells. Complexes were immunoprecipitated with anti-GFP antibody and co-precipitated proteins were detected with anti-GFP and anti-Myc antibodies. Numbers indicate amino acid positions in CEP152.

Figure S3, Related to Figure 3. Characterization of KIAA0753 and CCDC14 binding to CEP63

(A) GFP, GFP-CCDC14 or GFP-KIAA0753 was expressed and complexes were immunoprecipitated with anti-GFP antibody and co-precipitated proteins were detected with anti-GFP and anti-CEP63 antibodies. CEP63 antibody detects different isoforms of CEP63 in cellular extracts. The prominent band corresponds to isoform 3 of CEP63 (58 kDa). **(B)** Schematic of CEP63 full length (FL) and deletion constructs and summary of interactions with KIAA0753 and CCDC14. Interactions were determined by co-immunoprecipitation experiments as described in (C and D). Numbers indicate amino acid positions in CEP63. **(C and D)** Data for B. GFP-CEP63 (FL), truncation protein constructs, or GFP vector control were co-expressed with Myc-CCDC14 or Myc-KIAA0753. Complexes were immunoprecipitated with anti-GFP antibody and co-precipitated proteins were detected with anti-GFP and anti-Myc antibodies.

Figure S4, Related to Figure 4. Specificity of KIAA0753 and CCDC14 antibodies and RNAi phenotypes

(A) U2OS cells were fixed 48 h after transfection with control siRNA, KIAA0753 siRNA or CCDC14 siRNA, and stained for KIAA0753 or CCDC14. DNA was stained with DAPI. Cells are outlined in white. **(B)** U2OS cells were co-transfected with the indicated siRNA and expression constructs. GFP-KIAA0753^{RR} represents RNAi-resistant allele. Cells were fixed after 48 h and stained with antibodies to GFP and centrin. **(C)** Quantification of B. **(D)** U2OS cells were co-transfected with the indicated siRNA and expression constructs and arrested in S phase by hydroxyurea treatment for 48 h. Cells were stained with antibodies to GFP and centrin. **(E)** Quantification of D. (**F)** U2OS cells were co-transfected with the indicated siRNA and expression constructs. GFP-CCDC14^{RR} represents RNAi-resistant allele. Cells were fixed after 48 h and stained with antibodies to GFP and centrin. **(G)** Quantification of F. Data in C, E, G represent mean value from three experiments per condition, +/- SEM; n≥75 cells per experiment. Scale bars = 10 μm, all insets show 4x enlarged centrosomes.

Table S1. Related to Figure 2. Proximity interactors of PLK4, CEP192, CEP63, CCDC67, CEP152 and CPAP

Mass spectrometry analysis of proximity interactors of the indicated Myc-BirA* fusion proteins. Note that for CEP152 two constructs were used, one in which Myc-BirA* is fused to the N-terminus (BirA*-CEP152) and the other in which Myc-

BirA* is fused to the C-terminus (CEP152-BirA*). Proximity interactors are ranked in the order of their NSAF values (average of three independent experiments). Proteins in black were previously shown to localize to the centrosome and proteins in bold were shown to interact physically with the corresponding centrosome protein in published data or in this work.

Table S2. Related to Figure 4. Proximity interactors of KIAA0753 and CCDC14

Mass spectrometry analysis of proximity interactors of Myc-BirA*-KIAA0753 and Myc-BirA*-CCDC14. Proximity interactors are ranked in the order of their NSAF values (average of three independent experiments). Proteins in black were previously shown to localize to the centrosome and proteins in bold were previously shown to be centriolar satellite proteins in published data or in this work.

Supplemental Experimental Procedures

Cell culture and transfection

U2OS, and HEK293T cells were grown in DMEM (Invitrogen) supplemented with 10% fetal bovine serum (FBS; Atlanta Biologicals, Lawrenceville, GA). All cells were cultured at 37 °C and 5% CO_2. U2OS cells were transfected with the plasmids using Lipofectamine LTX according to the manufacturer's instructions (Invitrogen). HEK293T cells were transfected with the plasmids using 1 μg/μl

polyethylenimine, MW 25 kDa (PEI, Sigma-Aldrich, St. Louis, MO). Briefly, the plasmids were diluted in Opti-MEM (Invitrogen), and incubated with PEI for 20 min at room temperature. The DNA/PEI complex was added to the cells and the culture medium was replaced with fresh medium after 4 h of incubation with the transfection mix. For microtubule-depolymerization experiments, cells were treated with 5 μg/ml nocodazole (US Biological, Swampscott, MA) or vehicle (dimethyl sulfoxide) for 3 h at 37 °C.

Plasmids

Full-length cDNAs of CEP63 (GenBank/EMBL/DDBJ accession no. NM_001042383.1), PLK4 (accession no. NM_014264), CEP152 (accession no. NM_001194998), CCDC67 (accession no. BC096547.1), CPAP (accession no. BC113664.1), CEP192 (accession no BC144481.1), PLK4 (accession no. NM_014264), CDK5RAP2 (accession no BC143762.1) were obtained from Open Biosystems. Full-length cDNAs of CCDC14 (BC040285.1) and KIAA0753 (BC113016.1) were obtained from DF/HCC DNA Resource Core (Harvard Medical School, MA). The ORFs of these genes were amplified by PCR and N-terminally tagged with BirA* by cloning into pcDNA3.1-mycBioID [S1]. CEP152 and CEP63 were also C-terminally tagged with BirA* by cloning into pcDNA3.1-Myc-BirA*. The ORFs of CEP63, CCDC14 and KIAA0753 were amplified by PCR and cloned into pDONR221 using the Invitrogen Gateway system. Subsequent Gateway recombination reactions using pCS2+6xMyc DEST provided by M.

Nachury (Stanford University, Stanford, CA) and pcDNA-DEST47 (Invitrogen) were used to generate Myc-CEP63, GFP-CEP63, Myc-CCDC14, GFP-CCDC14, Myc-KIAA0753 and GFP-KIAA0753. Full-length and deletion constructs of CEP152 were described previously [S2]. Deletions constructs of CEP63 were made by PCR amplification of the indicated regions. PCR products were cloned into pDONR221 and gateway recombination reactions using pcDNA-DEST47 were used to produce GFP-tagged deletion constructs. siRNA resistant CCDC14 and KIAA0753 clones (CCDC14^{RR} and KIAA0753^{RR}) were generated by making five consecutive synonymous base pair changes in the center of the siRNA targeted region using overlapping PCR with the primers 5′- ggttcattctgaagtt caaactgatggcaaTagCcaAttCgcTtcacaaggtaaaacagtttctgc -3′ and 5′- catcagta caggttgcagaaactgttttaccttgtgaAgcGaaTtgGctAttgccatcagtttgaac -3′ for CCDC14; and 5′-tgcgccgaatggaagagatggaaaaataccaggaAtcAgtAcgAcaGagatataata aaatcgcatatgctgatcctcgac -3′ and 5′-ttcctgcatccaaagtcgaggatcagcatatgcg attttattatatctCtgTcgTacTgaTtcctggtatttttccatctc-3′ for KIAA0753. PCR products were cloned into pDONR221 and gateway recombination reactions using pcDNA-DEST47 were used to produce GFP- CCDC14^{RR} and GFP- KIAA0753^{RR}.

RNAi and rescue experiments

CCDC14 was depleted using an siRNA with the sequence 5′- TGGCAACAGTCA GTTTGCATCACAA-3′. KIAA0753 was depleted using an siRNA with the sequence 5′- CCAGGAGTCTGTTCGTCAAAGATAT -3′. PCM1 was depleted

using an siRNA with the sequence 5′-GGGCTCTAAACGTGCCTCC -3′ as previously described [S3]. CEP63 was depleted using an siRNA with the sequence 5′- GGCTCTGGCTGAACAATCATT -3′ as previously described [S4]. CEP152 was depleted using pool of two siRNA duplexes 5′-GCGGATCCAACTGGAAATCTA-3′ and 5′-GCATTGAGGTTGAGACTAA-3′ as previously described [S2]. CDK5RAP2 was depleted using an siRNA with the sequence 5′-TGGAAGATCTCCTAACTAA-3′ as described previously [S5]. A GC-rich scrambled siRNA with the sequence 5′-AAACTAAACTGAGGCAATGCC -3′ was used as a control. All siRNAs were synthesized by Invitrogen. siRNAs were transfected into U2OS cells using Lipofectamine RNAiMax following manufacturer's instructions (Invitrogen). For rescue experiments, U2OS cells were cotransfected with siRNA and the expression plasmids (GFP, GFP-CCDC14^{RR} or GFP-KIAA0753^{RR}) using Oligofectamine (Invitrogen) following manufacturer's instructions and cells were fixed and stained after 48 h.

Antibodies

Anti-PCM1 antibody was obtained by immunizing rabbits (Cocalico Biologicals, Reamstown, PA) with GST-tagged human PCM-1 comprising amino acids 1665-2026 purified from *Escherichia coli*. The antibody was affinity purified against MBP-PCM1 (aa 1665-2026) and used at 0.5 ug/ml for immunofluorescence. Polyclonal rabbit anti-CCDC14 (Genetex) and anti-KIAA0753 (Sigma) were used

at 1:1000 for immunofluorescence. Other antibodies used for immunofluorescence in this study were goat anti-PCM1 (Santa Cruz), mouse anti-γ-tubulin (GTU-88; Sigma-Aldrich) at 1:4000, mouse anti-GFP (3e6; Invitrogen at 1:750, mouse anti-centrin3 (Abnova) at 1:2000, mouse anti-Myc (9e10; Sigma-Aldrich) at 1:500, rabbit anti-CEP63 (Milipore) at 1:2000, rabbit-CDK5RAP2 (Abcam) and rabbit anti-CEP152 (Bethyl) at 1:1000. Antibodies used for western blotting were mouse anti-Myc (9e10; Sigma-Aldrich) at 1:2000, rabbit rabbit anti-GFP at 0.15 μg/ml (as previously described in [S2]) and rabbit anti-CEP63 (Milipore) at 1:1000.

Immunoprecipitation

For the co-immunoprecipitation experiments, HEK293T cells were transiently transfected, incubated for 24 h, washed with PBS, and lysed in lysis buffer (50 mM Tris, pH 7.4, 266 mM NaCl, 2.27 mM KCl, 1.25 mM KH_2PO_4, 6.8 mM Na_2HPO_4-$7H_2O$ and 1% NP-40, protease inhibitors). Insoluble material was pelleted, and soluble material was incubated with goat anti-GFP antibodies (Rockland) and then with protein A beads (Affi-Prep). Beads were washed in lysis buffer, eluted in sample buffer, and run on SDS-PAGE gels.

Biotin-streptavidin affinity purification

For the BioID experiments, HEK293T cells were transfected with BirA*-tagged proteins. 24 h post-transfection, transfected cells were supplemented with 50 μM

biotin and incubated a futher 18 h. For CEP192, PLK4, CEP63, CCDC67, CEP152 and CPAP, centrosome-enriched fractions were prepared from these cells by sucrose gradient centrifugation as described previously [S6]. Briefly, cells were treated with 5 μg/ml nocodazole and cytochalasin B for 1 h at 37 °C. Cells were then lysed in lysis buffer (20 mM HEPES, pH 7.8, 5 mM K-acetate, 0.5 mM $MgCl_2$, 0.5 mM DTT, protease inhibitors), dounce homogenized and centrifuged at 2500 g for 5 min. The resulting supernatant was then centrifuged on a discontinuous sucrose gradient (70, 50, and 40% sucrose) at 26,000 g for 1 h. Gradient fractions were collected from the top, centrosome fractions were pooled and lysed at 25 °C in lysis buffer (50 mM Tris, pH 7.4, 500 mM NaCl, 0.4% SDS, 5 mM EDTA, 1 mM DTT, 2% Triton X-100, protease inhibitors) and sonicated. For CCDC14 and KIAA0753, after transfection with BirA*-tagged proteins and biotin treatment, cells were directly lysed in lysis buffer. An equal volume of 4 °C 50 mM Tris (pH 7.4) was added to the extracts and insoluble material was pelleted. Soluble materials from whole cell lysates and centrosome enriched extracts were incubated with Dynabeads (MyOne Streptavidin C1; Invitrogen) overnight. Beads were collected and washed twice in wash buffer 1 (2% SDS in dH2O), once with wash buffer 2 (0.2% deoxycholate, 1% Triton X-100, 500 mM NaCl, 1 mM EDTA, and 50 mM Hepes, pH 7.5), once with wash buffer 3 (250 mM LiCl, 0.5% NP-40, 0.5% deoxycholate, 1% Triton X-100, 500 mM NaCl, 1 mM EDTA and 10 mM Tris, pH 8.1) and twice with wash buffer 4 (50 mM Tris, pH 7.4, and 50 mM NaCl). 10% of the sample was reserved for Western blot

analysis and 90% of the sample to be analyzed by mass spectrometry was washed twice in 50 mM NH_4HCO_3.

Mass spectrometry

Proteins bound to beads were reduced by 20-minute incubation with 5 mM TCEP (*tris*(2-carboxyethyl)phosphine) and alkylated in the dark by treatment with 10mM Iodoacetamide for 20 additional minutes. The proteins were subsequently digested by adding Sequencing Grade Modified Trypsin (Promega, Madison, WI, USA) and placing the reaction mixture in a Thermomixer (Eppendorf, Westbury, NY) and incubating overnight at 37 °C at 750 rpm. The next day, the sample was acidifed with formic acid to a final concentration of 5% and spun at 14,000 rpm for 30 min. The supernatant was carefully transferred to a separate microfuge tube so as not to disturb the bead pellet, and pressure-loaded into a biphasic trap column.

MS analysis of the samples was performed using MudPIT technology [S7]. Capillary columns were prepared in-house from particle slurries in methanol. An analytical column was generated by pulling a 100 µm ID/360 µm OD capillary (Polymicro Technologies, Inc., Phoenix, AZ) to 3 µm ID tip. The pulled column was packed with reverse phase particles (Aqua C18, 3 µm dia., 90 Å pores, Phenomenex, Torrance, CA) until 15 cm long. A biphasic trapping column was prepared by creating a Kasil frit at one end of an undeactivated 250 µm ID/360 µm OD capillary (Agilent Technologies, Inc., Santa Clara, CA), which was then

successively packed with 2.5 cm strong cation exchange particles (Partisphere SCX, 5 µm dia., 100 Å pores, Phenomenex, Torrance, CA) and 2.5 cm reverse phase particles (Aqua C18, 5 µm dia., 90 Å pores, Phenomenex, Torrance, CA). The trapping column was equilibrated using buffer A (5% acetonitrile/0.1% formic acid) prior to sample loading. After sample loading and prior to MS analysis, the resin-bound peptides were desalted with buffer A by letting it flow through the trap column. The trap and analytical columns were assembled using a zero-dead volume union (Upchurch Scientific, Oak Harbor, WA).

LC–MS/MS analysis was performed on LTQ Orbitrap or LTQ Orbitrap Velos (Thermo Scientific, San Jose, CA, USA) interfaced at the front end with a quaternary HP 1100 series HPLC pump (Agilent Technology, Santa Clara, CA, USA) using an in-house built electrospray stage. Electrospray was performed directly from the analytical column by applying the ESI voltage at a tee (150 µm ID, Upchurch Scientific) directly downstream of a 1:1000 split flow used to reduce the flow rate to 250 nL/min through the columns. A fully automated 6-step MudPIT run was performed on each sample using a three mobile phase system consisting of buffer A (5% acetonitrile/0.1% formic acid), buffer B (80% acetonitrile/0.1% formic acid), and buffer C (500 mM ammonium acetate/5% acetonitrile/0.1% formic acid). The first step was 60 min reverse-phase run, whereas five subsequent steps were of 120 min duration with different concentration of buffer C run for 4 min at the beginning of each of the gradient. In LTQ Orbitrap Velos, peptides were analyzed using a Top-20 data-dependent

acquisition method in which fragmentation spectra are acquired for the top 20 peptide ions above a predetermined signal threshold. As peptides were eluted from the microcapillary column, they were electrosprayed directly into the mass spectrometer with the application of a distal 2.4 kV spray voltage. For each cycle, full–scan MS spectra (*m/z* range 300-1600) were acquired in the Orbitrap with the resolution set to a value of 60,000 at *m/z* 400 and an automatic gain control (AGC) target of 1×10^6 ions and the maximal injection time of 250 ms. For MS/MS scans the target value was 10,000 ions with injection time of 25 ms. Once analyzed, the selected peptide ions were dynamically excluded from further analysis for 120 s to allow for the selection of lower-abundance ions for subsequent fragmentation and detection using the setting for repeat count = 1, repeat duration = 30 ms and exclusion list size = 500. Charge state filtering, where ions with singly or unassigned charge states were rejected from fragmentation was enabled. The minimum MS signal for triggering MS/MS was set to 500 and an activation time of 10 ms were used. All tandem mass spectra were collected using normalized collision energy of 35%, an isolation window of 2 Th. In LTQ Orbitrap, peptides were analyzed using a Top-10 data-dependent acquisition method.

For protein identification we used Integrated Proteomics Pipeline (IP2, San Diego, CA) software, a web-based proteomics data analysis platform that supports both cloud and cluster computing, developed by Integrated Proteomics Applications, Inc. (http://www.integratedproteomics.com/). Tandem mass spectra

were extracted from the Xcalibur data system format (.raw) into MS2 format using RawXtract1.9.9.2. The MS/MS spectra were searched with the ProLuCID algorithm against the EBI human IPI database (version 3.71, release date March 24, 2010) that was concatenated to a decoy database in which the sequence for each entry in the original database was reversed. The database also had sequence for two proteins, *E. coli* BirA-R118G and mouse CCDC67, appended to it. The search parameters include 50 ppm peptide precursor mass tolerance and 0.6 Da for the fragment mass tolerance acquired in the ion trap. The initial wide precursor mass tolerance in the database search was subjected to postsearch filtering and eventually constrained to 20 ppm. Carbamidomethylation on cysteine was defined as fixed modification and phosphorylation on STY was included as variable modification in the search criteria. The search space also included all fully– and semi–tryptic peptide candidates of length of at least six amino acids. Maximum number of internal miscleavages was kept unlimited, thereby allowing all cleavage points for consideration. ProLuCID outputs were assembled and filtered using the DTASelect2.0 program that groups related spectra by protein and removes those that do not pass basic data-quality criteria [S8]. DTASelect2.0 combines XCorr and ΔCN measurements using a quadratic discriminant function to compute a confidence score to achieve a user-specified false discovery rate (less than 1% in this analysis).

Data analysis for Mass Spectrometry

For each BioID experiment data presented in the table or network format in this study, data were derived from three biological replicates. Control data were derived from 3 independent experiments of mock-transfected and BirA*-transfected HEK293T cells. To compare data across different runs and assess the abundance of each proximity partner, we applied the normalization of spectral counts [S9]. Because larger proteins are expected to generate more spectral counts than smaller proteins, the number of spectral counts for each protein was divided by the protein's length, defining the spectral abundance factor (SAF). To account for variability between independent runs, individual SAF values were normalized against the sum of all SAFs for a particular run, resulting in normalized SAF (NSAF). NSAF values range from 0 to 1 but for presentation purposes, we multiplied each NSAF value by 1000, thus NSAF values for each particular run range from 0 to 1000. To distinguish the nonspecific interactions from the specific ones, we calculated the ratio of the NSAF of each identified protein to the NSAF of this protein in control datasets. A protein was considered a contaminant if the ratio was greater than 2.5. The proteins that were estimated to be a mass spectrometry contaminant by the contaminant repository for affinity purification-mass spectrometry data [S10] in HEK293T cells were also selected out as contaminant proteins. For the analysis of the data from three independent BioID experiments, we only accounted for the proteins that were identified in at least 2 independent experiments and that have a spectral count greater than 4. In the case of proteins with multiple isoforms, the largest isoform was chosen to

assign spectral count for these proteins. The numbers presented in the tables are average NSAF values of three independent experiments.

Immunofluorescence, microscopy and quantitation

For immunofluorescence experiments, cells were grown on coverslips and fixed in methanol for indirect immunofluorescence. After rehydration in PBS, cells were blocked in 3% BSA (Sigma-Aldrich) in PBS + 0.1% Triton X-100. Coverslips were incubated in primary antibodies diluted in blocking solution as previously indicated (see Antibodies), and Alexa Fluor 488-, 594-, or 680-conjugated secondary antibodies were diluted in 1:500 in blocking solution (Invitrogen). Biotinylated proteins were detected with streptavidin coupled to Alexa Fluor 594 (1:500; Invitrogen). Samples were mounted using Mowiol mounting medium containing N-propyl gallate (Sigma-Aldrich). Coverslips of cells were imaged using OpenLab software (version 4.0.4; Perkin-Elmer) on a microscope (Axiovert 200M; Carl Zeiss, Inc.) with Plan Neofluar 100X 1.3 NA objectives. In addition, coverslips were imaged by spinning disk confocal microscopy using a Zeiss Axiovert with a Yokogawa CSU-10 confocal head. Images were captured using a cooled charge-coupled device camera (Orca ER, Hamamatsu Photonics; Cascade EM-CCD, Photometrics) and were processed using Photoshop (Adobe).

Quantitative immunofluorescence for CEP152, CDK5RAP2 and CEP63 was performed on cells by acquiring a z-stack of control and depleted cells using

identical gain and exposure settings, determined by adjusting settings based on the fluorescence signal in the control cells. The z-stacks were used to assemble maximum-intensity projections. The centrosome regions in these images were defined by γ-tubulin staining for each cell. Average pixel intensity of fluorescence within the region of interest was measured using ImageJ (National Institutes of Health, Bethesda, MD). Background subtraction was performed by quantifying fluorescence intensity of a region of equal dimensions in the area neighboring the centrosome.

Statistical analysis

Statistical significance and p values were assessed by analysis of variance and Student's *t* tests using Prism software (GraphPad Software, La Jolla, CA). Error bars reflect SEM. Following key is followed for asterisk placeholders for *p*-values in the figures: ***p<0.001, **p<0.01, *p<0.05.

Supplemental References

S1. Roux, K.J., Kim, D.I., Raida, M., and Burke, B. (2012). A promiscuous biotin ligase fusion protein identifies proximal and interacting proteins in mammalian cells. J Cell Biol *196*, 801-810.

S2. Hatch, E.M., Kulukian, A., Holland, A.J., Cleveland, D.W., and Stearns, T. (2010). Cep152 interacts with Plk4 and is required for centriole duplication. J Cell Biol *191*, 721-729.

S3. Dammermann, A., and Merdes, A. (2002). Assembly of centrosomal proteins and microtubule organization depends on PCM-1. J Cell Biol *159*, 255-266.

S4. Loffler, H., Fechter, A., Matuszewska, M., Saffrich, R., Mistrik, M., Marhold, J., Hornung, C., Westermann, F., Bartek, J., and Kramer, A. (2011). Cep63 recruits Cdk1 to the centrosome: implications for regulation of mitotic entry, centrosome amplification, and genome maintenance. Cancer Res *71*, 2129-2139.

S5. Fong, K.W., Choi, Y.K., Rattner, J.B., and Qi, R.Z. (2008). CDK5RAP2 is a pericentriolar protein that functions in centrosomal attachment of the gamma-tubulin ring complex. Mol Biol Cell *19*, 115-125.

S6. Tsou, M.F., and Stearns, T. (2006). Mechanism limiting centrosome duplication to once per cell cycle. Nature *442*, 947-951.

S7. Washburn, M.P., Wolters, D., and Yates, J.R., 3rd (2001). Large-scale analysis of the yeast proteome by multidimensional protein identification technology. Nat Biotechnol *19*, 242-247.

S8. Tabb, D.L., McDonald, W.H., and Yates, J.R., 3rd (2002). DTASelect and Contrast: tools for assembling and comparing protein identifications from shotgun proteomics. J Proteome Res *1*, 21-26.

S9. Zybailov, B., Mosley, A.L., Sardiu, M.E., Coleman, M.K., Florens, L., and Washburn, M.P. (2006). Statistical analysis of membrane proteome

expression changes in Saccharomyces cerevisiae. J Proteome Res *5*, 2339-2347.

S10. Mellacheruvu, D., Wright, Z., Couzens, A.L., Lambert, J.P., St-Denis, N.A., Li, T., Miteva, Y.V., Hauri, S., Sardiu, M.E., Low, T.Y., et al. (2013). The CRAPome: a contaminant repository for affinity purification-mass spectrometry data. Nat Methods *10*, 730-736.